JGR Atmospheres

RESEARCH ARTICLE
10.1029/2020JD033399

Key Points:

- We found a net deposition trend from air to water, which is different from the trends in other marginal seas of China
- Northeastern China was the main source of polycyclic aromatic hydrocarbons (PAHs) in the air masses in this season, and PAHs were carried mainly by gas phase

Supporting Information:

Supporting Information may be found in the online version of this article.

Correspondence to:

X. Zou and C. Wang,
zouxq@nju.edu.cn;
clwang@nju.edu.cn

Citation:

Feng, Z., Wang, C., Zhang, C., Wang, W., Wang, J., Li, Y., & Zou, X. (2021). Air-water exchange and gas-particle partitioning of polycyclic aromatic hydrocarbons (PAHs) in coral reef areas of the South China Sea. *Journal of Geophysical Research: Atmospheres*, *126*, e2020JD033399. https://doi.org/10.1029/2020JD033399

Received 1 JUL 2020
Accepted 21 APR 2021

Air-Water Exchange and Gas-Particle Partitioning of Polycyclic Aromatic Hydrocarbons (PAHs) in Coral Reef Areas of the South China Sea

Ziyue Feng[1,2,3], Chenglong Wang[1,2,3,4], Chuchu Zhang[1,2,3], Wanzhi Wang[1,2,3], Jiajia Wang[3], Yali Li[1,2,3], and Xinqing Zou[1,2,3]

[1]Ministry of Education Key Laboratory for Coast and Island Development, Nanjing University, Nanjing, China, [2]Collaborative Innovation Center of South China Sea Studies, Nanjing University, Nanjing, China, [3]School of Geographic and Oceanographic Sciences, Nanjing University, Nanjing, China, [4]Yuxiu Postdoctoral Institute, Nanjing University, Nanjing, China

Abstract In this study, we collected gas, particulate, and surface water-dissolved phase samples from 16 sites in the South China Sea from March 21 to April 12, 2018. Thereafter, all the samples were analyzed for the air-water exchange and source apportionment of polycyclic aromatic hydrocarbons (PAHs). Thus, it was observed that the overall PAH concentrations in the water and gas phases were 8.0 ± 5.5 ng/L and 41.3 ± 24.7 ng/m^3, respectively. Back trajectory simulation showed that the air masses in the South China Sea primarily originated from mainland China during the heating period, and air-water exchange analysis showed net deposition from air to water, with fluxes ranging from −5.53 to −89.72 ng/m^2/d. Further, the logarithmic gas-particle partitioning coefficient (logK_p) of the PAHs regressed linearly with the logarithmic subcooled liquid vapor pressure (log P0 L), with an average slope of −0.3 ± 0.13.

1. Introduction

Polycyclic aromatic hydrocarbons (PAHs) are a form of persistent organic pollutants that are distributed worldwide (Masclet et al., 1995; Yu et al., 2017). Based on United States Environmental Protection Agency regulation, 16 kinds of priority-controlled PAHs, including naphthalene (Nap), acenaphthylene (Acy), acenaphthene (Ace), fluorene (Flu), phenanthrene (Phe), anthracene (Ant), fluoranthene (Flo), pyrene (Pyr), benzo(a)anthracene (BaA), chrysene (Chr), benzo(b)fluoranthene (BbF), benzo(k)fluoranthene (BkF), benzo(a)pyrene (BaP), indeno (1,2,3-cd)pyrene (IndP), benzo (g,hi)perylene (BghiP), and dibenzo (a,h)anthracene (DahA), are considered to present risks to human health. Further, several kinds of human activities and natural processes, including petroleum leakage, the incomplete combustion of wood or fossil fuels, and biological consolidation diagenesis (Simoneit, 2002; Yunker et al., 1996), can lead to the release of PAHs.

Marginal seas have become some of the most important sinks for PAHs (Jiang et al., 2018; Wang et al., 2017), owing to input processes, including riverine transport, dry and wet deposition, and shipping activities (Parinos et al., 2013; Yunker et al., 2002), and in some areas far from land, airborne deposition may be the main input method.

The South China Sea is the largest (3.5 million km^2 surface area) and deepest of China's three major marginal seas. Influenced by the East Asian monsoon and surrounded by developing countries, such as China, Vietnam, the Philippines, and Malaysia, this sea receives large amounts of contaminants originating from industrial activities as well as other human activities. For instance, 8,092 t/y of PAHs have been transported out of mainland China into its marginal seas, with the South China Sea receiving 991 t/y (Lang et al., 2008). Although many researchers have assessed PAH contamination in the Bohai, Yellow, East, and northern South China Seas (Chen et al., 2016; Luo et al., 2008; B. Li et al., 2012), few have focused on the reef areas in the southern South China Sea.

Coral reefs are productive and highly biodiverse shallow-water ecosystems that are essential for the survival of several organisms (Y. Li et al., 2019; Ranjbar et al., 2018). However, the influence of organic contaminants on them has become one of the most important factors bringing about their bleaching (Y. Li et al., 2019; Xiang et al., 2018). As coral reefs in the South China Sea are not directly affected by coastal contaminant sources, such as runoff and industrial sewage, the main nonpoint source of PAHs in this area may

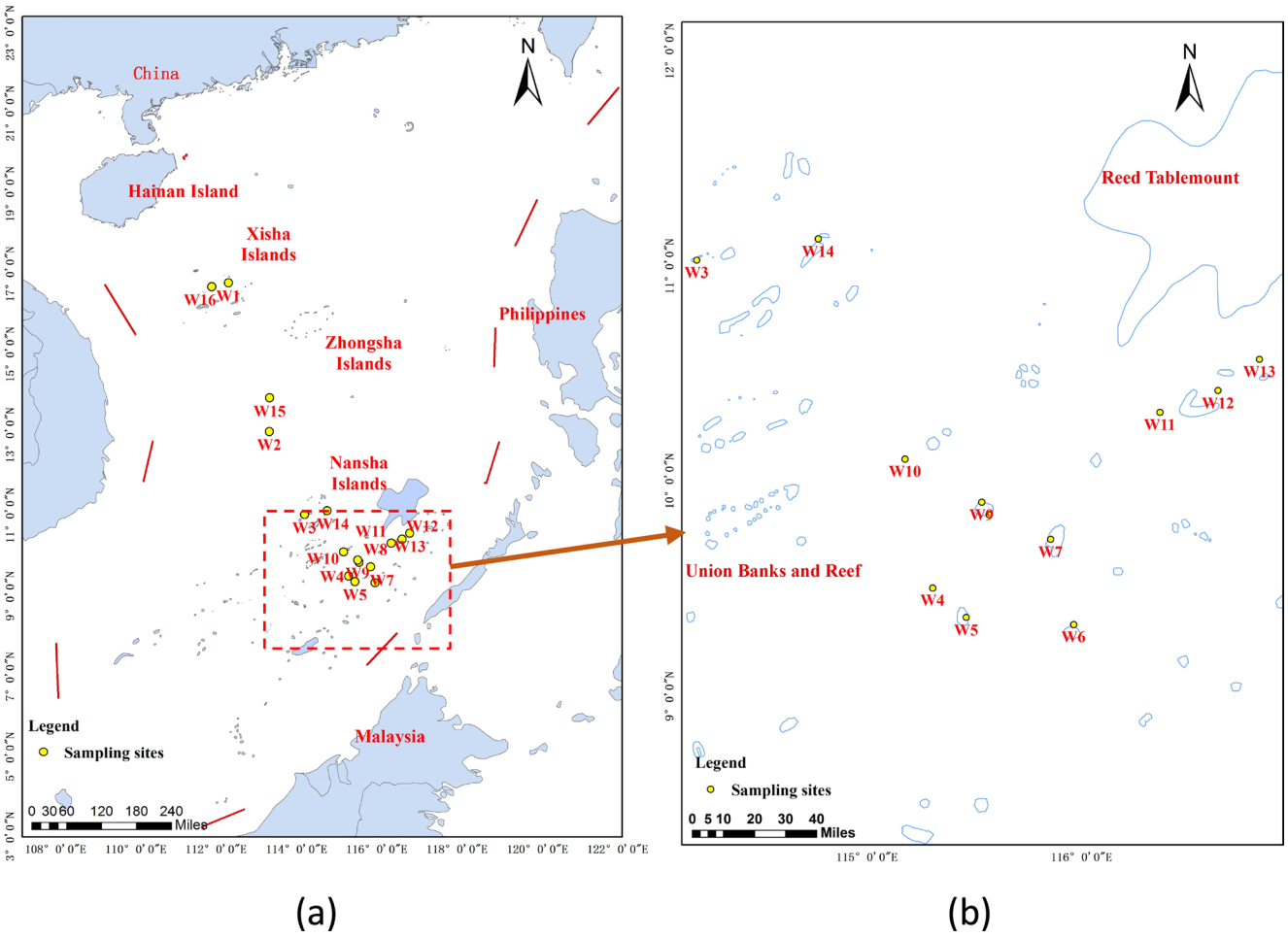

Figure 1. (a) Map of sampling sites (both water and air). (b) Enlarged map of sampling sites in the Nansha Islands.

be atmospheric inputs. It has also been reported that air-water exchange fluxes can be used to determine the dynamics of contaminant transport and distinguish the role of air/sea sources and sinks.

In this study, we assessed the concentration and spatial distribution of PAHs in water and gas in reef areas of the South China Sea to: (1) determine the status of PAH pollution in this area, (2) calculate the direction and flux of PAH air-water exchange, and (3) calculate the gas-particle partitioning of PAHs.

2. Materials and Methods

2.1. Sample Collection

We collected 16 surface water samples (2 L each) and 16 gas samples at 24-h intervals from the Xisha Islands to the Nansha Islands in the South China Sea from March 21 to April 12, 2018 (Figure 1). The air samples (gas and particulate phases) were collected using active air samplers (Tisch TE-1000 polyurethane foam [PUF] samplers, Shanghai Yiwin instrument and equipment) that were placed above the forecastle of the campaign vessel. The air sampler was well removed from potential contamination sources, such as the ship's stack/exhaust, and was operated only under a prevailing headwind. The gas samples were collected using polyurethane foam (PUF) plugs, and were extracted using n-hexane (HPLC grade, Tedia, USA) for 48 h before analysis. Further, the particulate phases were collected on quartz microfiber filters (QM-A, Whatman). These plugs and filters were stored in opaque plastic bags and kept frozen at 253 K until analysis.

The water samples were collected using a polymethyl methacrylate water collector (2 L) during the air sample collection. Before each water sample was collected, the collector was cleaned twice using surface water. Thereafter, five kinds of deuterated PAHs (Nap-D8, Ace-D10, Phe-D10, Chr-D12, and Pyr-D12) were added into each bottle as recovery surrogates. The collected water samples were then forced through a 0.7 μm precombusted glass fiber filter (GF/F, Whatman) using a circulating water vacuum pump to remove the particulate phase. These filtered water samples were then kept frozen at 253 K until laboratory analysis. After sample collection, the air and water samples were transported to laboratory and extracted within 2 days.

2.2. Sample Preparation and Analysis

Dissolved PAHs were absorbed using C18 solid phase extraction columns (Supelclean ENVI-18, Supelco) that were activated using 2 × 3 ml n-hexane, 2 × 3 ml dichloromethane, and 2 × 3 ml acetone. Thereafter, the C18 solid phase extraction columns were eluted twice using 1.5 and 3 ml of acetone and dichloromethane, respectively. The PUF plugs and filters were Soxhlet-extracted using dichloromethane for 48 h, and the extracts as well as the elutions were purified using a 20-ml solution containing n-hexane and dichloromethane in the ratio 1:1 20 ml in columns with silica gel, aluminum oxide, and anhydrous copper sulfate. Thereafter, they were concentrated via rotary evaporation and the solvent was replaced with n-hexane in 1 ml for analysis.

All the PAH in the samples were identified via gas chromatography/triple quadrupole mass spectrometry (GC-MS, Thermo Fisher Scientific, TSQ 8000 Evo, USA) using a quartz capillary TG-5MS column (30 m × 0.25 mm × 0.25 μm film thickness). The injection volume was 1 μL in spiltless mode. The solvent delay time was 5 min and high purity helium, at a flow rate of 1 mL/min, was used as the carrier gas. The heating procedure was as follows: the initial temperature was set at 70°C, followed by heating to 140°C at a heating rate of 25°C/min after holding for 1 min, then heating to 240°C at a heating rate of 10°C/min, and finally, heating to 300°C at a heating rate of 5°C/min after holding for 4 min. The PAH quantification process was performed in accordance with the external standard procedure and the values obtained were corrected using the recovery surrogates (Nap-D8, Ace-D10, Phe-D10, Chr-D12, and Pyr-D12).

2.3. Quality Control

Field blanks and laboratory blanks (solvent only) were used to calibrate the data corresponding to both the air and dissolved phases for every four-sample set. Specifically, air phase field blanks were obtained by exposing the sampling media to air for a few seconds, and water phase field blanks were obtained by filling the collection bottles with ultrapure water. Laboratory blanks were obtained for every four samples during sample preparation using ultrapure water, C18 solid phase extraction columns, and precleaned PUF plugs and filters. Naphthalene was not analyzed and reported in this study owing to its volatility and low recovery. Further, the target compounds in laboratory and field blanks showed minimal levels (below detection limit), demonstrating that the samples were not contaminated during processing or transportation. Known concentrations of five recovery surrogates (Nap-D8, Ace-D10, Phe-D10, Chr-D12, Pyr-D12) were added to the PUF plugs and filters, as well as water before the samples were frozen. This was to enable the calculation of the recoveries of the 15 PAHs in both water and air. The recoveries of the surrogates in air and the particulate phase were 50 ± 6% and 56 ± 4% for Nap-D8, 83 ± 7% and 81 ± 8% for Ace-D10, 94 ± 9% and 92 ± 12% for Phe-D10, 126 ± 15% and 130 ± 13% for Chr-D12, and 118 ± 11% and 125 ± 12% for Pyr-D12, respectively. In the water phase, they were 68 ± 5, 90 ± 8, 99 ± 6, 101 ± 9, and 106 ± 11% for Nap-D8, Ace-D10, Phe-D10, Chr-D12, and Pyr-D12, respectively. The method detection limit (MDL), which was calculated as the mean of the field blank plus three times the standard deviation, were 0.01–0.25 pg/m^3 for the air samples and 0.01–0.12 pg/L for the water samples.

2.4. Fugacity Fractions and Air-Water Exchange Flux Calculation

Fugacity fractions, which were calculated according to Equations 1–3 below (Bidleman et al., 2016), were used to describe the directions of air-water exchange fluxes.

$$f_{\text{water}} = C_{\text{water}} H \quad (1)$$

$$f_{\text{air}} = C_{\text{air}} RT \tag{2}$$

$$FR = \frac{f_{\text{water}}}{f_{\text{air}}} \tag{3}$$

where f_{water} and f_{air} represent the PAH fugacities in water and air, respectively; C_{air} and C_{water} represent gaseous and dissolved PAH concentrations, respectively; and FR is the ratio of f_{water} to f_{air}. FR < 1 means net deposition from air to water, $FR = 1$ suggests a dynamic equilibrium between air and water, and $FR > 1$ means net volatilization.

We calculated the air-water exchange flux using the two-layer film model (Whitman, 1923) that has been employed in several other studies (Bamford et al., 1999; Cheng et al., 2013; Schwarzenbach et al., 2003; Z. Wu et al., 2017). The functioning of the air-water exchange flux is related to the mass transfer coefficient and the PAH concentrations in the water and air phases as follows:

$$F = K_{ol}\left(C_{water} - C_{air} RT \,/\, H\right) \tag{4}$$

where F (ng/m^2/d) represents the air-water exchange, K_{ol} (m/d) is the total mass transfer coefficient, R (8.314 Pa (/m^3/mol/d)) is the gas constant, H is the dimensionless Henry's law constant for PAHs, and T (K) is the absolute temperature. K_{ol} was calculated using the mass transfer coefficient in water and air:

$$\frac{1}{K_{ol}} = \frac{1}{K_{water}} + \frac{RT}{K_{air} H} \tag{5}$$

where K_{water} and K_{air} are the mass transfer coefficients of the water and air phases, respectively. The calculation of K_{water} and K_{air} are provided in the Supporting Information Text 2.4

2.5. Uncertainty for Each Flux Estimation

The uncertainty corresponding to the estimation of each flux was calculated using a widely used error propagation analysis method derived from Shoemaker et al. (1974), which has been used in several studies (Bamford et al., 1999; Cheng et al., 2013; Liu et al., 2016; Nelson et al., 1998). The error caused by random uncertainty was be calculated as follows:

$$\sigma^2\left(F\right) = \left(\frac{\partial F}{\partial K_{ol}}\right)^2 \left(\sigma K_{ol}\right)^2 + \left(\frac{\partial F}{\partial C_w}\right)^2 \left(\sigma C_W\right)^2 + \left(\frac{\partial F}{\partial C_a}\right)^2 \left(\sigma C_a\right)^2 \tag{6}$$

In our calculations, the error coefficients corresponding to C_{w} and C_{a} were estimated to be 20% based on the measured replicate samples and the surrogate recoveries. Further, to cover the uncertainties in the air and water mass transfer coefficients as well as wind speed, the error value for K_{ol} was assumed to be 40% (Bamford et al., 1999; Cheng et al., 2013; Nelson et al., 1998).

The overall propagated error associated with the calculation of the PAH air-water exchange fluxes ranged between 8% and 684% with a mean of 110%. Our result was a little higher than those reported by Fang et al., (2008) (51%) and Bamford et al., (1999) (64%), but were close to that reported by Cheng et al., (2013) (102%). Higher percent errors were associated with smaller fluxes and K_{ol} variations, given that it was the only variable that was not measured directly (Bamford et al., 1999; Cheng et al., 2013; Fang et al., 2008; Nelson et al., 1998).

2.6. Back Trajectory Simulation

Back trajectories were used to simulate the source and running path of the air mass. The HYSPLIT Trajectory Ensemble model of the National Oceanic and Atmospheric Administration (https://www.ready.noaa.gov/HYSPLIT_traj.php) was used to determine the origin of the air mass at several heights and dates for up to 120 h. With this model, it is also possible to start new trajectories at 1-h intervals. For the ensemble to

realize configuration optimally, the starting height should be greater than 250 m. Thus, we used 120 h and a height of 300 m to calculate the back trajectories for W1 (close to Hainan Island), W2 (middle of the study area), and W9 (middle of the Nansha Islands) so as to represent the characteristics of these three regions.

2.7. Gas-Particle Partitioning of PAHs

As important as air-water exchange, gas-particle partitioning plays a crucial role in the study of remote seas (Y. Yang et al., 2010). PAHs are partitioned into both the gas and particles phases, depending on influential factors, such as temperature, particulate characteristics, and the type of chemicals present on the particulates (Lohmann et al., 2000; Pankow, 1994). Numerous models of organic matrix absorption and particle surface adsorption have been reported (Dachs & Eisenreich, 2000; Finizio et al., 1997; Harner & Bidleman, 1998; Pankow, 1994).

The partitioning coefficient, K_p, was calculated as follows:

$$K_p = \left(C_p \,/\, \mathrm{TSP}\right) / C_a \tag{7}$$

where C_p and C_a are the PAH concentrations (ng/m^3) in the particulate and gas phases, respectively, and TSP represents the concentration of total suspended particulate matter (μg/m^3). A linear relationship between logK_p and log P0 L (P0 L represent the compound's subcooled liquid-vapor pressure, Pa) for nonpolar organic compounds has been established (Pankow, 1994) as:

$$\log K_p = m_r \log P_L^0 + b_r \tag{8}$$

where m_r and b_r are fitting constants corresponding to logK_p and log P0 L, respectively. In this study, TSP and P0 L data were collected from previous studies (Lei et al., 2002; Paasivirta et al., 1999; Shi et al., 2010).

3. Results and Discussion

3.1. PAHs in the Surface Water-Dissolved Phase and Air

3.1.1. PAHs in the Surface Water-Dissolved Phase

The concentrations of 10 PAHs (excluding those of BbF, BkF, IndP, DahA, and BghiP, which were below the DLs) in the surface water-dissolved phase ranged from 1.94 (W13) to 22.6 ng/L (W2), with an average of 8.0 ± 5.5 ng/L. According to Figure 2, the highest values were observed in the area between Xisha (W1, W16) and Nansha Islands (W3–W14), where the channels are dense. It has been reported that coral reefs are more common in areas with low PAHs content. T. Yang et al. (2019) observed good linear correlations between PAH contents in seawater and sediments. However, Xiang et al. (2018) reported a poor correlation between the biota-sediment accumulation factor and hydrophobicity, indicating that PAHs in corals possibly bioaccumulate from seawater. The study conducted by Ko et al. (2014) indicated that corals have higher levels of PAHs than ambient surface sediments. In this study, the input of PAHs primarily depended on atmospheric deposition. Therefore, corals may lead to the lower levels of PAHs in the seawater in the reef seas. The PAH concentrations rose south of the Nansha Islands, possibly because of nearby human activity and river inputs from Malaysia. Our results on the concentrations of PAHs in the water phase are much lower than those obtained in previous studies conducted in the Bohai sea (16 PAHs, 267.0 ng/L) (Tong et al., 2019) and the Yellow sea (16 PAHs, 109.4 ng/L) (Han et al., 2009). Although our study area is the biggest marginal sea of China, the pollution level of the water is still limited owing to the lack of runoff inputs. Flo, Ant, and Ace accounted for 41.4%, 13.4%, and 10.5% of the total PAH concentration, respectively. Obviously, the dissolved PAHs were dominated by low molecular weight (LMW) PAHs, with relatively high vapor pressures and higher solubilities (logK_{ow}: 3.9–4.6) (McDonough et al., 2014).

3.1.2. PAH Concentrations in the Gas Phase

In total, 14 PAHs, except BkF, with concentration below the DL, were present in the gas phase. These 14 PAHs showed concentrations ranging from 18.0 (W13) to 113.1 ng/m^3 (W6), with an average of 41.3 ± 24.7 ng/m^3.

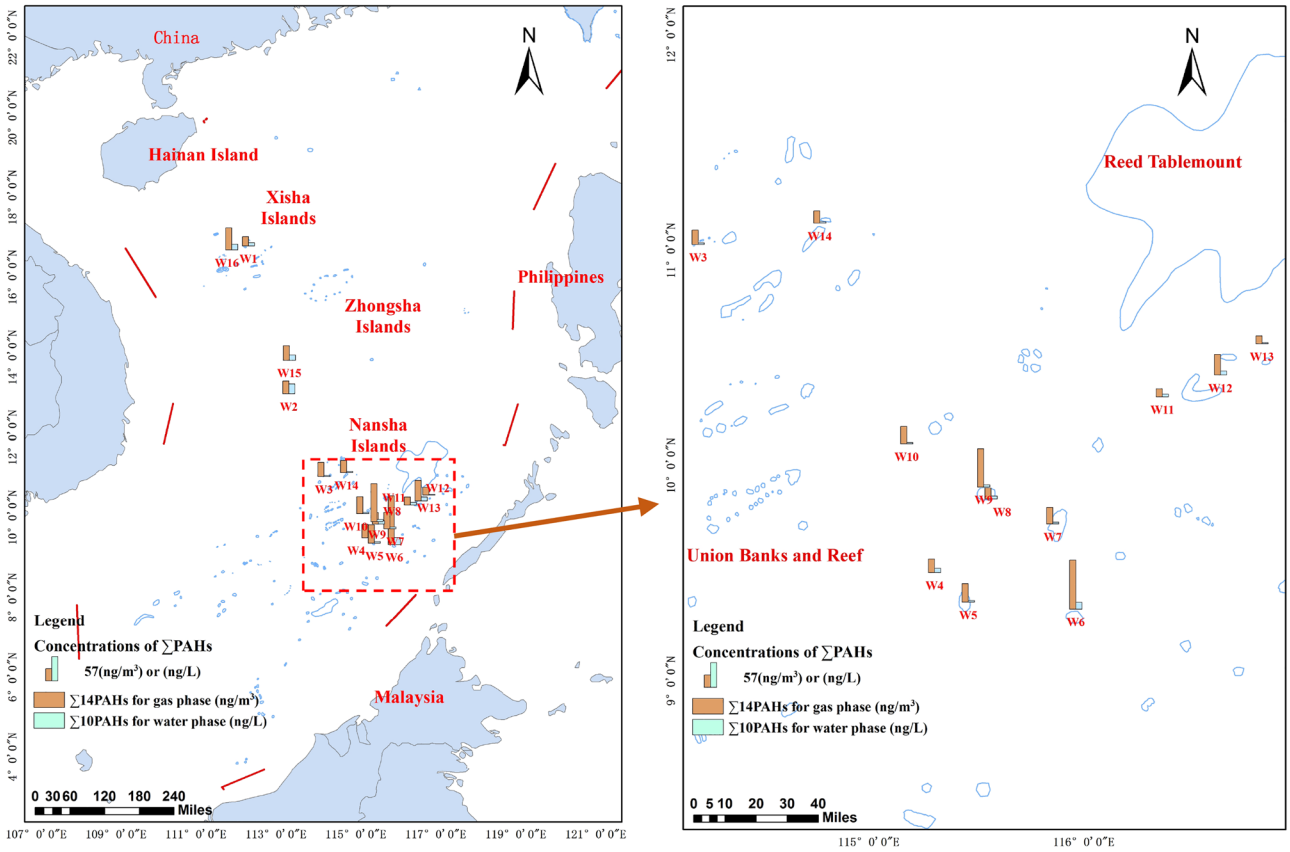

Figure 2. Concentrations of ΣPAHs in water phase and gas phase. PAHs, polycyclic aromatic hydrocarbons.

Additionally, in the particulate phase, 14 PAHs were also observed, showing concentrations ranging from 0.2 (W14) to 3.7 ng/m^3 (W6), with an average of 0.8 ± 0.8 ng/m^3. Further, in gas phase, the predominant PAHs were Phe (46.8%), Flu (25.7%), and Pyr (13.7%), accounting for 86.2% of the total concentration of the PAHs. The congener patterns in the air at the study sites were similar to those in Dalian, located in northeastern China (Phe: 45%, Flu: 16%) (X. Wu et al., 2019) and Korea (Phe: 37%, Flu: 21%) (Kim & Chae, 2016). It was also observed that Phe and Flu were dominant in the gas phase, owing to their relatively high vapor pressures. In accordance with Figure 3b, higher PAH concentrations were predominantly distributed in the southern Nansha Islands (W3–W14). Furthermore, considering the characteristics of the East Asian monsoon, in which the air mass over the South China Sea is mainly derived from the northeast, a major portion of these airborne contaminants possibly originated from mainland China. Regarding the neighboring countries, still-developing Southeast Asian countries are likely to produce higher levels of contaminants; thus, the PAHs in the air over the South China Sea possibly originated from these surrounding regions.

To study the air mass sources more accurately, back trajectories were used to simulate the source and running path of the air masses. Figure 4 shows the results of the back trajectory ensemble simulation near Hainan Island (W1), in the middle of the study area (W2), and in the middle of the Nansha Islands (W9). It was evident that under the influence of the East Asian monsoon in spring, the direction of the transportation of the air masses in all the three areas was northeast. The air masses in W1 display high similarity in source and were routed from the Korean Peninsula to mainland China before reaching Hainan Island. Additionally, those in W2 were similar to those in W1, that is, were also routed from the Korean Peninsula to mainland China. Combined with the previous discussion regarding the concentration of PAHs in the gas phase, the lower PAH concentrations in the gas phase in Hainan Islands (W1) and the middle part of the study area (W2) may be due to the forest filtration effect on mainland China (Su & Wania, 2005). The air masses in W9 (Figure 4c), which represent those over all of the Nansha Islands, were all sourced at different heights from the western Pacific, even though those at lower heights were also influenced by the northern

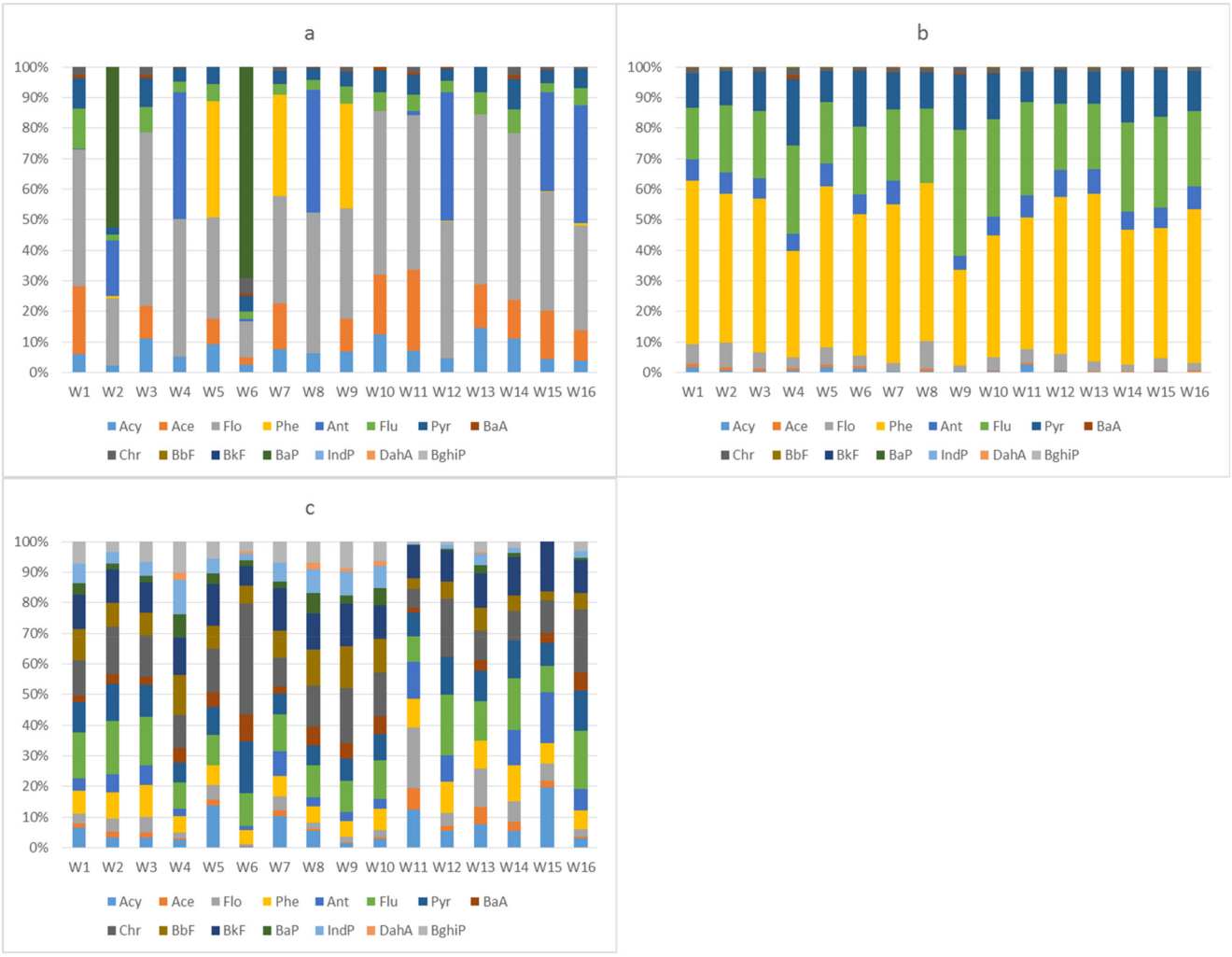

Figure 3. Polycyclic aromatic hydrocarbons (PAH) profiles for the (a) water phase, (b) gas phase, and (c) particulate phase.

Philippines. However, according to Figure 3, all 16 sites showed similar PAH compositions. Thus, all the samples might have been influenced by a major strong pollution source. Further, considering the Chinese heating period (burning fossil fuels to provide central heating for city dwellers in northern China from October to April) and Figures 4a and 4b, we performed another simulation (Figure 4d) to extend the results shown in Figure 4c. In accordance with Figure 4d, some of the air masses in the Nansha Islands (W9) directly originated from northeastern China, while others originated from the Korean Peninsula and northeastern China, then went through Japan. A previous study showed that the PAH content of the air in Japan is higher during the Chinese heating period (X. Y. Yang et al., 2007), and this can be primarily attributed to the transportation of PAHs from northeastern China. Therefore, the concentrations of PAHs in the air over the South China Sea were mainly influenced by northeastern China and those in the air over the Korean Peninsula by the East Asian monsoon.

3.2. Fugacity Ratio and Air–Water Exchange Fluxes

Using the equations defined in Section 2.3, we calculated the PAH fugacity ratio at the 16 sampling sites, as shown in Table S4, and it was observed that net deposition occurred at all the sites. González-Gaya et al., (2016) reported a net deposition in the subtropical and tropical Atlantic, Pacific, and Indian oceans. Conversely, net volatilization owing to the discharge of heavily polluted coastal runoff (the Yellow River and the Yangtze River) and the longer half-lives in the water-dissolved phase, have been observed in another

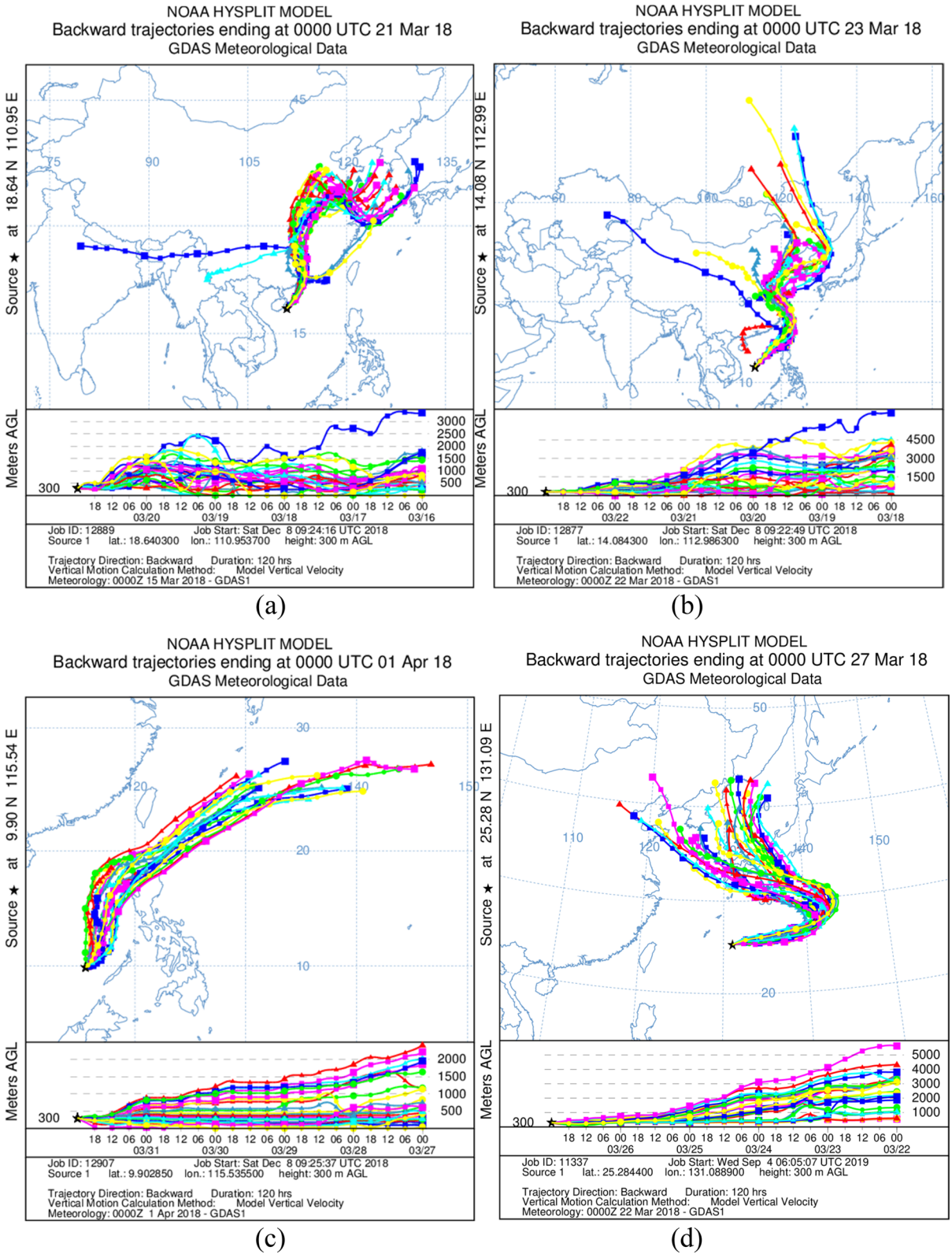

Figure 4. (a, b) 120 h backward trajectories of air masses in W1 and W2 and (c, d) 240 h backward trajectories of air masses in W9.

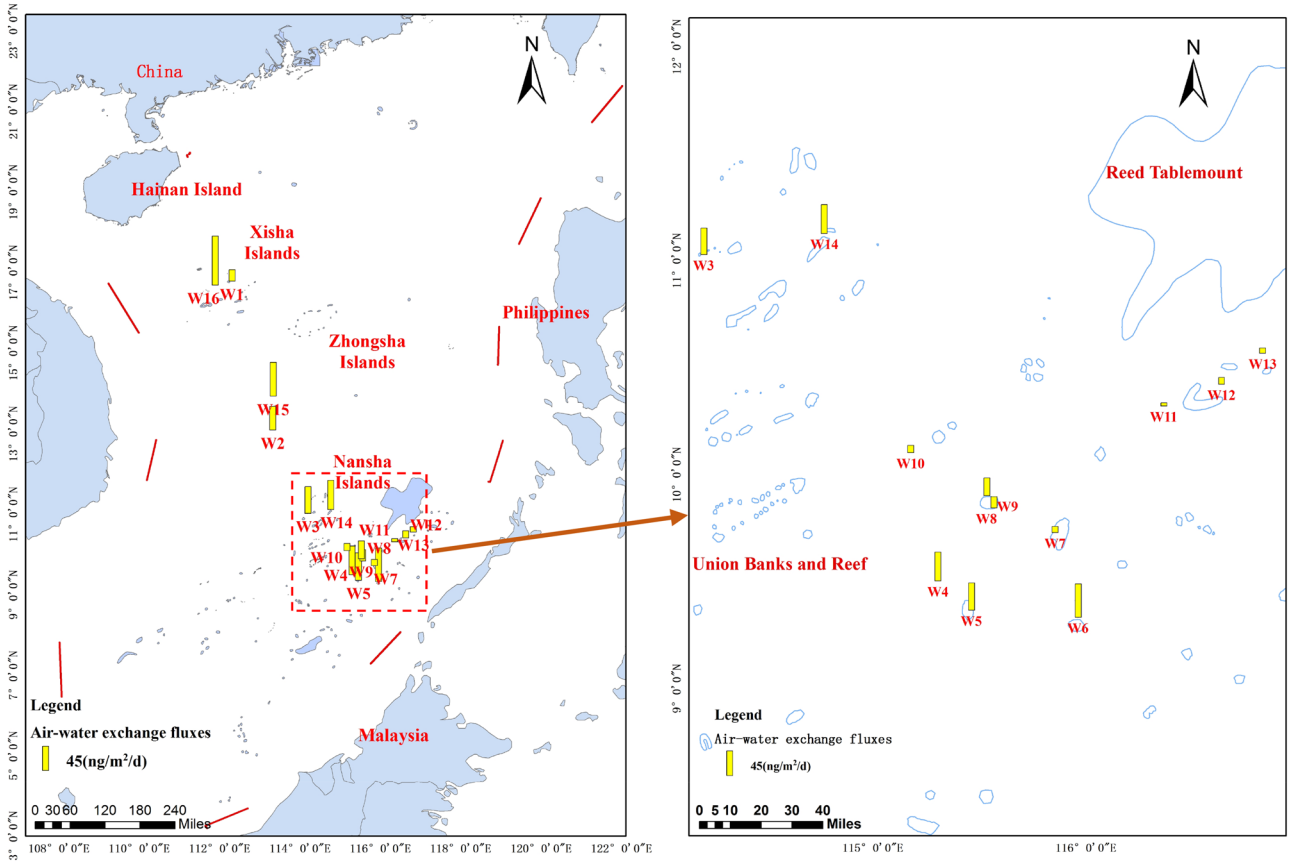

Figure 5. Air-water exchange fluxes of 15 polycyclic aromatic hydrocarbons (PAHs) in the study area.

China marginal seawater (Bohai Sea and Yellow Sea) (Chen et al., 2016; Mackay & Callcott, 1998). Further, Lohmann et al. (2011) observed that in coastal areas, most PAHs show net volatilization; however, PAH adsorption occurred in the farther area of the bay. Compared with the results of the previous studies mentioned above, it was observed net volatilization generally occurred in coastal areas with heavily polluted runoff or polluted industrial sources. In this study, it was observed that the South China Sea is not directly influenced by coastal runoff or large nearby industrial PAH sources. Therefore, this phenomenon may be caused by the lower PAH concentrations in the water owing to limited coastal runoff inputs.

The calculated air-water exchange fluxes are shown in Figure 5. The values ranged from −5.53 (W11) to −89.72 ng/m^2/d (W16) with an average of −36.70 ± 23.7 ng/m^2/d; the negative values represent net deposition from air to water. The distribution of the exchange fluxes showed that the sampling sites in the west had higher values than those in the east; this may be related to the dynamic conditions of this area, such as the East Asian monsoon and ocean currents. As was the case with the percentages of the airborne PAHs shown in Figure 2, the exchange fluxes of Phe (−9.91 ng/m^2/d), Flu (−14.46 ng/m^2/d), and Pyr (−6.66 ng/m^2/d), which accounted for 27%, 39%, and 18% of the total exchange fluxes, respectively, were higher than those of the other PAHs.

3.3. Gas-Particle Partitioning of PAHs

The mass fraction, θ ($C_{particle}/C_{particle} + C_{gas}$), of all the PAHs, which ranged between 0.001 and 1.000, with an average of 0.411, indicating that most of the PAHs were in the particulate phase. It was also observed that θ increased as the number of benzene rings in the PAHs increased, and was ~1 for several high-molecular weight PAHs. At similar temperatures, regions under the influence of nearby urban and industrial sources had higher θ values (Mandalakis et al., 2002; Mulder et al., 2014). The linear regressions of logK_p and log

P0 L for the 14 PAHs (except BkF) that were present in all the samples were obtained, and it was observed that the slopes for 16 samples ranged from ~−0.08 to −0.53 with the average of −0.30 ± 0.13. It was also observed that the slopes obtained in this study are shallower than some reported in previous studies conducted in southeast China (S.-P. Wu et al., 2014; Y. Yang et al., 2010), but similar to those reported in studies conducted in the northwest Pacific Ocean (Z. Wu et al., 2017). The slopes deviated from −1, indicating that the phase distribution was not at theoretical equilibrium. Further, deviations from the equilibrium value of −1 have possibly been attributed to a nonexchange ability, the continuous input of freshly emitted PAHs, the slow gas-to-particle sorption of PAHs, the diffusion and mixing processes of air masses underwent over the South China Sea (Pankow & Bidleman, 1991; S.-P. Wu et al., 2014; Z. Wu et al., 2017), or the lower TSP and higher concentrations of PAHs in the gas phase. A slope steeper than −1 suggests the predominance of adsorption, while a slope shallower than −0.6 indicates the predominance of absorption, and slopes ranging between −0.6 and −1 correspond to absorption and adsorption (Goss et al., 1998). In this study, all the samples showed slopes that were shallower than −0.6, indicating that absorption was predominant. According to Table S9, the higher $\log K_p$ of the lower molecular weight compounds (Nap, Acy, Ace, and Flo) brought about the observed shallower slopes for all the sampling sites. As already mentioned above, the entire sampling area was experiencing net deposition, and the East Asian monsoon transported large amounts of PAHs from northwest China during heating-period via air masses. Thus, the continuous input of freshly emitted PAHs and the lower concentration of TSP possibly brought the gas-particle partitioning into a state of disequilibrium, and the contribution of PAHs in the particulate phase was very limited.

4. Conclusions

In this study, we investigated PAH concentrations in airborne and water-dissolved phases within the coral reef areas in the South China Sea and calculated the air-water exchange fluxes as well as source apportionment. A net deposition trend from air to water, which is different from the trends in other marginal seas, such as the Yellow Sea and Bohai Sea, but similar to those in the major oceans around the world, was observed. Back trajectory simulations indicated that northeastern China is the main source of PAHs in the air masses corresponding to this season, and judging from the air-water exchange fluxes as well as the results of gas-particle partitioning analyses, PAHs have been continuously imported into reef areas via the gas phase. Under these conditions, there should be more concern regarding the exposure of corals to PAHs and more attention should be paid to atmospheric PAH inputs as a possible source of PAH contamination in corals.

Data Availability Statement

The data for this study are publicly accessible on the Zenodo repository (https://zenodo.org/record/4281618#.X7cjf_nDWLk).

Acknowledgments
This study was supported by the Marine Science and Technology Innovation Project of Jiangsu Province (Grant HY2018-9), the Fundamental Research Funds for the Central Universities (Grant 14380001), and the National Science Foundation of China (Grant 41471431).

References

Bamford, H. A., Poster, D. L., & Baker, J. E. (1999). Temperature dependence of Henry's law constants of thirteen polycyclic aromatic hydrocarbons between 4°C AND 31°C. *Environmental Toxicology & Chemistry*, *18*, 1905–1912. https://doi.org/10.1002/etc.5620180906

Bidleman, T. F., Agosta, K., Andersson, A., Haglund, P., Liljelind, P., Hegmans, A., et al. (2016). Sea-air exchange of bromoanisoles and methoxylated bromodiphenyl ethers in the northern baltic. *Marine Pollution Bulletin*, *112*, 58–64. https://doi.org/10.1016/j.marpolbul.2016.08.042

Cheng, J.-O., Ko, F.-C., Lee, C.-L., & Fang, M.-D. (2013). Air-water exchange fluxes of polycyclic aromatic hydrocarbons in the tropical coast, Taiwan. *Chemosphere*, *90*, 2614–2622. https://doi.org/10.1016/j.chemosphere.2012.11.020

Chen, Y., Lin, T., Tang, J., Xie, Z., Tian, C., Li, J., et al. (2016). Exchange of polycyclic aromatic hydrocarbons across the air–water interface in the bohai and yellow seas. *Atmospheric Environment*, *141*, 153–160. https://doi.org/10.1016/j.atmosenv.2016.06.039

Dachs, J., & Eisenreich, S. J. (2000). Adsorption onto aerosol soot carbon dominates gas-particle partitioning of polycyclic aromatic hydrocarbons. *Environmental Science and Technology*, *34*. https://doi.org/10.1021/es991201+

Fang, M., Ko, F., Baker, J., & Lee, C. (2008). Seasonality of diffusive exchange of polychlorinated biphenyls and hexachlorobenzene across the air-sea interface of Kaohsiung Harbor, Taiwan. *The Science of the Total Environment*, *407*, 548–565. https://doi.org/10.1016/j.scitotenv.2008.09.021

Finizio, A., Mackay, D., Bidleman, T., & Harner, T. (1997). Octanol-air partition coefficient as a predictor of partitioning of semi-volatile organic chemicals to aerosols. *Atmospheric Environment*, *31*, 2289–2296. https://doi.org/10.1016/s1352-2310(97)00013-7

González-Gaya, B., Fernández-Pinos, M.-C., Morales, L., Méjanelle, L., Abad, E., Piña, B., et al. (2016). High atmosphere–ocean exchange of semivolatile aromatic hydrocarbons. *Nature Geoscience*, *9*(6). 438–442, https://doi.org/10.1038/ngeo2714

Goss, K.-U., & Schwarzenbach, R. P. (1998). Gas/solid and gas/liquid partitioning of organic compounds: Critical evaluation of the interpretation of equilibrium constants. *Environmental Science & Technology*, *32*, 2025–2032. https://doi.org/10.1021/es9710518

Han, B., Jiang, F., Li, P., Zhang, X., Song, Z., & Wang, X. (2009). Distribution and origin of polycyclic aromatic hydrocarbons in the sea water, pore water and sediment of the central area in the South Yellow Sea (in Chinese). *Advances in Marine Science*, *2*.

Harner, T., & Bidleman, T. F. (1998). Octanol-air partition coefficient for describing particle/gas partitioning of aromatic compounds in urban air. *Environmental Science & Technology*, *32*, 1494–1502. https://doi.org/10.1021/es970890r

Jiang, Y., Lin, T., Wu, Z., Li, Y., Li, Z., Guo, Z., & Yao, X. (2018). Seasonal atmospheric deposition and air-sea gas exchange of polycyclic aromatic hydrocarbons over the Yangtze River Estuary, East China Sea: Implications for source-sink processes. *Atmospheric Environment*, *178*, 31–40. https://doi.org/10.1016/j.atmosenv.2018.01.031

Kim, S.-K., & Chae, D. H. (2016). Seasonal variation in diffusive exchange of polycyclic aromatic hydrocarbons across the air-seawater interface in coastal urban area. *Marine Pollution Bulletin*, *109*, 221–229. https://doi.org/10.1016/j.marpolbul.2016.05.078

Ko, F.-C., Chang, C.-W., & Cheng, J.-O. (2014). Comparative study of polycyclic aromatic hydrocarbons in coral tissues and the ambient sediments from Kenting National Park, Taiwan. *Environmental Pollution*, *185*, 35–43. https://doi.org/10.1016/j.envpol.2013.10.025

Lang, C., Tao, S., Liu, W., Zhang, Y., & Simonich, S. (2008). Atmospheric transport and outflow of polycyclic aromatic hydrocarbons from China. *Environmental Science & Technology*, *42*, 5196–5201. https://doi.org/10.1021/es800453n

Lei, Y. D., Chankalal, R., Chan, A., & Wania, F. (2002). Supercooled liquid vapor pressures of the polycyclic aromatic hydrocarbons. *Journal of Chemical & Engineering Data*, *47*(4), 801–806. https://doi.org/10.1021/je0155148

Li, B., Feng, C., Li, X., Chen, Y., Niu, J., & Shen, Z. (2012). Spatial distribution and source apportionment of pahs in surficial sediments of the yangtze estuary, China. *Marine Pollution Bulletin*, *64*, 636–643. https://doi.org/10.1016/j.marpolbul.2011.12.005

Liu, Y., Wang, S., Mcdonough, C. A., Khairy, M., Muir, D. C. G., Helm, P. A., & Lohmann, R. (2016). Gaseous and freely-dissolved pcbs in the lower great lakes based on passive sampling: Spatial trends and air-water exchange. *Environmental Science & Technology*, *50*, 4932–4939. https://doi.org/10.1021/acs.est.5b04586

Li, Y., Wang, C., Zou, X., Feng, Z., Yao, Y., Wang, T., & Zhang, C. (2019). Occurrence of polycyclic aromatic hydrocarbons (PAHs) in coral reef fish from the South China Sea. *Marine Pollution Bulletin*, *139*, 339–345. https://doi.org/10.1016/j.marpolbul.2019.01.001

Lohmann, R., Dapsis, M., Morgan, E. J., Dekany, V., & Luey, P. J. (2011). Determining air-water exchange, spatial and temporal trends of freely dissolved pahs in an urban estuary using passive polyethylene samplers. *Environmental Science & Technology*, *45*, 2655–2662. https://doi.org/10.1021/es1025883

Lohmann, R., Northcott, G. L., & Jones, K. C. (2000). Assessing the contribution of diffuse domestic burning as a source of PCDD/FS, PCBS, and PAHS to the U.K atmosphere. *Environmental Science & Technology*, *34*. https://doi.org/10.1021/es991183w

Luo, X.-J., Chen, S.-J., Mai, B.-X., Sheng, G.-Y., Fu, J.-M., & Zeng, E. Y. (2008). Distribution, source apportionment, and transport of pahs in sediments from the Pearl River delta and the northern South China Sea. *Archives of Environmental Contamination and Toxicology*, *55*, 11–20. https://doi.org/10.1007/s00244-007-9105-2

Mackay, D., & Callcott, D. (1998). Partitioning and physical chemical properties of PAHs. In *The handbook of environmental chemistry: PAHs and related compounds* (pp. 325–345). Springer. https://doi.org/10.1007/978-3-540-49697-7_8

Mandalakis, M., Tsapakis, M., Tsoga, A., & Stephanou, E. G. (2002). Gas-particle concentrations and distribution of aliphatic hydrocarbons, PAHs, PCBs and PCDD/Fs in the atmosphere of Athens (Greece). *Atmospheric Environment*, *36*, 4023–4035. https://doi.org/10.1016/s1352-2310(02)00362-x

Masclet, P., Hoyau, V., Jaffrezo, J. L., & Legrand, M. (1995). Evidence for the presence of polycyclic aromatic hydrocarbons in the polar atmosphere and in the polar ice of greenland. *Analusis*, *23*, 250–252.

Mcdonough, C. A., Khairy, M. A., Muir, D. C. G., & Lohmann, R. (2014). Significance of population centers as sources of gaseous and dissolved pahs in the lower great lakes. *Environmental Science & Technology*, *48*, 7789–7797. https://doi.org/10.1021/es501074r

Mulder, M. D., Heil, A., Kukučka, P., Klánová, J., Kuta, J., Prokeš, R., et al. (2014). Air-sea exchange and gas-particle partitioning of polycyclic aromatic hydrocarbons in the Mediterranean. *Atmospheric Chemistry and Physics*, *14*, 8905–8915. https://doi.org/10.5194/acp-14-8905-2014

Nelson, E. D., Mcconnell, L. L., & Baker, J. E. (1998). Diffusive exchange of gaseous polycyclic aromatic hydrocarbons and polychlorinated biphenyls across the air-water interface of the Chesapeake Bay. *Environmental Science & Technology*, *32*, 912–919. https://doi.org/10.1021/es9706155

Paasivirta, J., Sinkkonen, S., Mikkelson, P., Rantio, T., & Wania, F. (1999). Estimation of vapor pressures, solubilities and Henry's law constants of selected persistent organic pollutants as functions of temperature. *Chemosphere*, *39*, 811–832. https://doi.org/10.1016/s0045-6535(99)00016-8

Pankow, J. F., & Bidleman, T. F. (1991). Effects of temperature, TSP and percent non-exchangeable material in determining the gas-particle partitioning of organic compounds. *Atmospheric Environment Part A. General Topics*, *25*, 2241–2249. https://doi.org/10.1016/0960-1686(91)90099-s

Pankow, J. F., & James, F. (1994). An absorption model of gas/particle partitioning of organic compounds in the atmosphere. *Atmospheric Environment*, *28*, 185–188. https://doi.org/10.1016/1352-2310(94)90093-0

Parinos, C., Gogou, A., Bouloubassi, I., Stavrakakis, S., Plakidi, E., & Hatzianestis, I. (2013). Sources and downward fluxes of polycyclic aromatic hydrocarbons in the open southwestern black sea. *Organic Geochemistry*, *57*, 65–75. https://doi.org/10.1016/j.orggeochem.2013.01.007

Ranjbar, J. A., Riyahi, B. A., Aliabadian, M., Laetitia, H., Shadmehri, T. A., & Yap, C. K. (2018). First report of bioaccumulation and bioconcentration of aliphatic hydrocarbons (PAHS) and persistent organic pollutants (PAHS, PCBS and PCNS) and their effects on alcyonacea and scleractinian corals and their endosymbiotic algae from the persian gulf, Iran: Inter and intra-species differences. *Science of the Total Environment*, *627*, 141–157. https://doi.org/10.1016/j.scitotenv.2018.01.185

Schwarzenbach, R. P., Gschwend, P. M., & Imboden, D. M. (2003). *Environmental Organic Chemistry* (2nd, pp. 906–937). Hoboken, NJ: Wiley.

Shi, J., Gao, H., Qi, J., Zhang, J., & Yao, X. (2010). Sources, compositions, and distributions of water-soluble organic nitrogen in particulates over the China Sea. *Journal of Geophysical Research*, *115*, D17303. https://doi.org/10.1029/2009jd013238

Shoemaker, D. P., Garland, G. W., & Steinfeld, J. I. (1974). Propagation of errors. *Experiments in physical chemistry* (pp. 51–58). New York, NY: McGraw-Hill.

Simoneit, B. R. T. (2002). Biomass burning: A review of organic tracers for smoke from incomplete combustion. *Applied Geochemistry*, *17*(3), 129–162. https://doi.org/10.1016/s0883-2927(01)00061-0

Su, Y., & Wania, F. (2005). Does the forest filter effect prevent semivolatile organic compounds from reaching the arctic? *Environmental Science & Technology*, *39*, 7185–7193. https://doi.org/10.1021/es0481979

Tong, Y., Chen, L., Liu, Y., Wang, Y., & Tian, S. (2019). Distribution, sources and ecological risk assessment of PAHs in surface seawater from coastal Bohai Bay, China. *Marine Pollution Bulletin*, *142*, 520–524. https://doi.org/10.1016/j.marpolbul.2019.04.004

Wang, C. L., Zou, X. Q., Zhao, Y. F., Li, Y. L., Song, Q. C., Wang, T., et al. (2017). Distribution pattern and mass budget of sedimentary polycyclic aromatic hydrocarbons in shelf areas of the eastern china marginal seas. *Journal of Geophysical Research: Oceans*, *122*. https://doi.org/10.1002/2017jc012890

Whitman, W. G. (1923). The two-film theory of gas absorption. *Chemical & Metallurgical Engineering*, *29*, 146–148.

Wu, S.-P., Yang, B.-Y., Wang, X.-H., Yuan, C.-S., & Hong, H.-S. (2014). Polycyclic aromatic hydrocarbons in the atmosphere of two subtropical cities in southeast china: seasonal variation and gas/particle partitioning. *Aerosol and Air Quality Research*, *14*, 1232–1246. https://doi.org/10.4209/aaqr.2013.01.0015

Wu, X., Wang, Y., Zhang, Q., Zhao, H., Yang, Y., Zhang, Y., et al. (2019). Seasonal variation, air-water exchange, and multivariate source apportionment of polycyclic aromatic hydrocarbons in the coastal area of Dalian, China. *Environmental Pollution*, *244*, 405–413. https://doi.org/10.1016/j.envpol.2018.10.075

Wu, Z., Lin, T., Li, Z., Jiang, Y., Li, Y., Yao, X., et al. (2017). Air-sea exchange and gas-particle partitioning of polycyclic aromatic hydrocarbons over the northwestern Pacific Ocean: Role of East Asian continental outflow. *Environmental Pollution*, *230*, 444–452. https://doi.org/10.1016/j.envpol.2017.06.079

Xiang, N., Jiang, C., Yang, T., Li, P., Wang, H., Xie, Y., et al. (2018). Occurrence and distribution of polycyclic aromatic hydrocarbons (PAHs) in seawater, sediments and corals from Hainan Island, China. *Ecotoxicology and Environmental Safety*, *152*, 8–15. https://doi.org/10.1016/j.ecoenv.2018.01.006

Yang, T., Cheng, H., Wang, H., Drews, M., Li, S., Huang, W., et al. (2019). Comparative study of polycyclic aromatic hydrocarbons (PAHs) and heavy metals (HMs) in corals, surrounding sediments and surface water at the Dazhou Island, China. *Chemosphere*, *218*, 157–168. https://doi.org/10.1016/j.chemosphere.2018.11.063

Yang, X. Y., Okada, Y., Tang, N., Matsunaga, S., Tamura, K., & Lin, J. M. (2007). Long-range transport of polycyclic aromatic hydrocarbons from China to Japan. *Atmospheric Environment*, *41*, 2710–2718. https://doi.org/10.1016/j.atmosenv.2006.11.052

Yang, Y., Guo, P., Zhang, Q., Li, D., Zhao, L., & Mu, D. (2010). Seasonal variation, sources and gas/particle partitioning of polycyclic aromatic hydrocarbons in Guangzhou, China. *The Science of the Total Environment*, *408*, 2492–2500. https://doi.org/10.1016/j.scitotenv.2010.02.043

Yu, C., Li, M., Cao, Y., Xian, H., Hong, Z., Zhang, T., et al. (2017). Source and yearly distribution of pahs in the snow from the hailuogou glacier of mountain Gongga, China. *Acta Geochimica*, *10*, 1–9. https://doi.org/10.1007/s11631-017-0231-x

Yunker, M. B., Macdonald, R. W., Vingarzan, R., Mitchell, R. H., Goyette, D., & Sylvestre, S. (2002). PAHs in the Fraser River basin: A critical appraisal of PAH ratios as indicators of PAH source and composition. *Organic Geochemistry*, *33*(4), 489–515. https://doi.org/10.1016/s0146-6380(02)00002-5

Yunker, M. B., Snowdon, L. R., Macdonald, R. W., Smith, J. N., Fowler, M. G., Skibo, D. N., et al. (1996). Polycyclic aromatic hydrocarbon composition and potential sources for sediment samples from the beaufort and barents seas. *Environmental Science & Technology*, *30*, 1310–1320. https://doi.org/10.1021/es950523k

Reference From the Supporting Information

Fuller, E. N., Schettler, P. D., & Giddings, J. C. (1966). New method for prediction of binary gas-phase diffusion coefficients. *Industrial & Engineering Chemistry Research*, *58*, 18–27. https://doi.org/10.1021/ie50677a007